Supporting Information

Rational design hybridized local and charge transfer emitters towards deep blue emission by incorporating extra cyano-based acceptor moiety

Xinjian Wang[1], Guimin Zhao[1], Tao Gao[2], Guanghao Zhang[1], Haowen Chen[1], Tao Zhou[1], Zhengmao Zhang[1], Wenwen Tian[1], Wei Jiang[1], Yueming Sun[1]*

1 Jiangsu Province Hi-Tech Key Laboratory for Bio-Medical Research, Jiangsu Engineering Laboratory of Smart Carbon-Rich Materials and Device, School of Chemistry and Chemical Engineering, Southeast University, Nanjing, Jiangsu, 211189, China.

2 Department of Chemistry, Bengbu No. 2 Middle School, Bengbu, Anhui, 233090, China.

*Corresponding author:

E-mail addresses: jiangw@seu.edu.cn (W. Jiang).

General Information

Materials and measurements

All reagents were purchased from commercial sources of chemical purity and used without additional purification. ^{1}H spectra and ^{13}C spectra were recorded on a Bruker Dex-600/150 NMR spectrometers in $CDCl_3$ solution. Molecular masses were measured by matrix-assisted laser desorption-ionization time-of-flight mass spectrometry (MALDI-TOF-MS) using a BRUKER DALTONICS instrument, with α-cyano-hydroxycinnamic acid as a matrix. Elemental analysis was determined by an Elementar Vario ELCHN elemental analyzer. UV–vis absorption and photoluminescence emission spectra were collected by a SHIMADZU UV-2600 spectrophotometer and a HORIBA FLUOROMAX-4 spectrophotometer, respectively. The low-temperature phosphorescence (PH) spectra were recorded on F-7000 FL spectrophotometer in toluene solution (10^{-5} M) by setting delay time (100 μs) and liquid nitrogen. Thermogravimetric analysis (TGA) and differential scanning calorimetry (DSC) curves were recorded with a NETZSCH TG 209F3 thermal analyzer (STA) system and NETZSCH DSC 214 modulated calorimeter under a dry N_2 gas flow at a heating rate of 10 °C min^{-1}. Cyclic voltammetry was performed using a CHI750C voltammetric analyzer with a scan rate of 100 mV/s at room temperature to investigate the oxidation potentials. A traditional three electrode cell was used as electrolytic cell, in which tetra-n-butylammonium hexafluorophosphate (Bu4NPF6) dissolving in dry CH2Cl2 solution (10^{-3} M) was employed as electrolyte. Platinum disk is used as the working electrode, platinum wire is regarded as the counter electrode and silver wire is used as the reference electrode. Ferrocenium/ferrocene (Fc/Fc+) is used as the external standard compound. The HOMO and LUMO levels were calculated according to the equations $E_{HOMO} = -(E_{onset,\ ox} + 4.4\ V)$, $E_{LUMO} = E_{HOMO} + E_g$, where E_{onset}, ox is the onset value of the first oxidation wave and E_g is the optical bandgap estimated from the absorption onset.

Theoretical computation method

Gaussian 09 software package was used for theoretical calculation. Geometry optimizations were conducted under the B3LYP/6-31G(d) level of theory. The ground

state geometries of compounds were optimized under B3LYP functional using density functional theory (DFT). In order to investigate the transition energies and the transition characters of the lowest excited singlet (S_1) and triplet states (T_1), time-dependent density functional theory (TD-DFT) method with B3LYP level, was carried out to calculate the energies of S_1, T_1, T_4, T_5 and singlet-triplet splitting energy (ΔE_{ST}). For the purpose of investigating the properties of excited-states, natural transition orbitals (NTOs) under B3LYP/6-31G(d) level were evaluated.

Device preparation process

OLED devices were fabricated using a clean glass substrate coated with an ITO layer as the anode, with a sheet resistance of 15 Ω cm^{-2} and an active pattern size of 2 × 2 mm^2. Before device fabrication, the ITO glass substrates were precleaned sequentially with deionized water, acetone and ethanol for three times to ensure the cleanliness of ITO surfaces. The PEDOT:PSS was directly spin-coated on an ITO plate and annealed at150 °C for 10 min. Sequentially, the configured EML solution was spin-coated onto the PEDOT:PSS layer and annealed at 80 °C for 10 min to remove the residual solvent under N_2 atmosphere. After the organic film was spin-coated, the TPBi, Cs_2CO_3, and Al were deposited consecutively onto the spin-coated film acting as the electron-transporting layer (ETL), electron-injection layer (EIL), and cathode. Finally, the device structure of ITO/PEDOT:PSS (40 nm)/EML (40 nm)/TPBi (40 nm)/Cs_2CO_3 (2 nm)/Al (100 nm) was obtained. The current density-voltage-luminance characteristics, current efficiency and power efficiency were tested using a Keithley 2400 Sourcemeter coupled with Si-potodiodes calibrated with PR655. The EL spectra were collected with a Photo-Research PR655 SpectraScan. All the device fabrication and characterization steps were carried out at room temperature under ambient laboratory conditions. External quantum efficiencies of the devices were calculated assuming a Lambertian emission distribution.

The Lippert-Mataga model calculation

The Lippert-Mataga model is estimated according to the following equations[1-3]:

$$hc(\upsilon_a - \upsilon_f) = hc\,(\upsilon^0_a - \upsilon^0_f) + \frac{2(\mu_e - \mu_g)^2}{a_0^3} f(\varepsilon,n)$$

Then take differential on both sides of equation:

$$\mu_e = \mu_g + \left\{\frac{hca_0^3}{2} + \left[\frac{d(\upsilon a - \upsilon f)}{df(\varepsilon,n)}\right]\right\}^{1/2}$$

where h is the Plank constant, c is the light speed in vacuum, f (ε,n) is the orientational polarizability of solvents and $f(\varepsilon,n) = \left[\frac{\varepsilon-1}{2\varepsilon+1} - \frac{n^2-1}{2n^2+1}\right]$, $\vartheta_a - \vartheta_f$ is the Stokes shifts when f is zero, a_0 is the solvent Onsager cavity radius, ε is the solvent dielectric constant and n is the solvent refractive index. The μe is the dipole moment of excited state and μ_g is the dipole moment of ground state, and μ_g can be estimated at the level of B3LYD/6-31g(d,p) with the Gaussian 09 package. The a_0 can be estimated with the relation: $a0 = (\frac{3M}{4N\pi d})^{1/3}$, in which M is the molar mass, N is the Avogadro's constant, and d is the density of solvent. The differential $\frac{d(\upsilon a - \upsilon f)}{df(\varepsilon,n)}$ can be estimated based on the photophysical data from the solvatochromic experiment.

Synthetic procedures

Synthesis of 3-([1,1':3',1''-terphenyl]-5'-yl)-9-phenyl-9H-carbazole (3ph-phCz)

Under nitrogen atmosphere, phCz-OB (1.11 g,3.0 mmol), 3ph-Br (1.10 g,3.6 mmol), K_2CO_3 (1.24 g,9.0 mmol) were added to a round-bottom flask, and tetrahydrofuran (24 mL) and water (6 mL) was added. After the mother liquor was replaced with nitrogen (N_2) for several times, $Pd(PPh_3)_4$ (0.35 g,0.3 mmol)were added quickly. The mixture was then heated at 80 °C and refluxed for 12 h. After cooling to room temperature, the mixture was filtered by diatomite and washed by chloromethane. The filtrate was collected and concentrated to get the crude product, which was then purified by column chromatography using dichloromethane/ petroleum ether (1:2, v/v) as the eluent. The target product was obtained as a white solid (1.26 g) with a yield of

89%.^{1}H NMR (600 MHz, $CDCl_3$): δ = 8.68 (d, J=1.5, 1H), 8.42 (d, J=7.7, 1H), 8.14 (d, J=1.5, 2H), 8.01 (s, 1H), 7.97-7.91 (m, 5H), 7.76-7.73 (m, 4H), 7.67 (dd, J=8.2, 3.6, 5H), 7.63-7.56 (m, 5H), 7.52-7.49 (m, 1H). ^{13}C NMR (150 MHz, $CDCl_3$): δ = 141.89, 141.19, 140.18, 140.15, 139.28, 136.40, 132.10, 128.73, 127.70, 126.34, 126.29, 126.25, 125.80, 125.06, 124.44, 124.19, 123.38, 122.80, 122.29, 119.28, 119.00, 117.85, 108.92, 108.78. MS (MALDI-TOF) [m/z]: Calcd for $C_{36}H_{25}N$, 471.20; Found, 471.21. Anal. Calcd for $C_{36}H_{25}N$: C, 91.69; H, 5.34; N, 2.97. Found: C, 91.70; H, 5.36; N, 2.94.

Synthesis of 5'-(9-phenyl-9H-carbazol-3-yl)-[1,1':3',1''-terphenyl]-2'-carbonitrile (3phCN-phCz)

3phCN-phCz was prepared according to the same procedure as that for 3ph-phCz, and the target product was obtained as a white solid (1.08 g) with a yield of 78%.^{1}H NMR (600 MHz, $CDCl_3$): δ = 8.47 (s, 1H), 8.23 (d, J=7.7, 1H), 7.86 (s, 2H), 7.76-7.72 (m, 5H), 7.66 (t, J=7.8, 2H), 7.61-7.56 (m, 6H), 7.52 (ddd, J=11.3, 7.6, 5.8, 4H), 7.47 (t, J=6.7, 2H), 7.36 (ddd, J=7.9, 6.2, 1.9, 1H). ^{13}C NMR (150 MHz, $CDCl_3$): δ = 146.29, 144.78, 140.40, 140.02, 137.88, 136.21, 129.81, 128.95, 128.04, 127.61, 126.73, 126.40, 125.96, 125.48, 124.26, 123.04, 122.12, 119.39, 118.18, 117.31, 109.32, 109.05, 106.98. MS (MALDI-TOF) [m/z]: Calcd for $C_{37}H_{24}N_2$, 496.19; Found, 496.12. Anal. Calcd. for $C_{37}H_{24}N_2$: C, 89.49; H, 4.87; N, 5.64. Found: C, 89.52; H, 4.91; N, 5.57.

Synthesis of 3,6-di([1,1':3',1''-terphenyl]-5'-yl)-9-phenyl-9H-carbazole (2(3ph)-phCz)

2(3ph)-phCz was prepared according to the same procedure as that for 3ph-phCz, and the target product was obtained as a white solid (1.34 g) with a yield of 73%. ^{1}H NMR (600 MHz, $CDCl_3$): δ = 8.54 (d, J=1.5, 2H), 7.94 (d, J=1.6, 4H), 7.80 (dt, J=3.2, 1.7, 4H), 7.78-7.75 (m, 8H), 7.69-7.65 (m, 4H), 7.54 (t, J=3.2, 4H), 7.52-7.50 (m, 8H), 7.43-7.39 (m, 4H). ^{13}C NMR (150 MHz, $CDCl_3$): δ = 141.91, 141.40, 140.32, 139.97, 136.51, 132.48, 129.01, 127.84, 126.66, 126.48, 126.41, 125.99, 124.82, 124.33, 123.61, 123.02, 118.12, 109.28. MS (MALDI-TOF) [m/z]: Calcd for $C_{54}H_{37}N$, 699.29; Found, 699.26. Anal. Calcd. for $C_{54}H_{37}N$: C, 92.67; H, 5.33; N, 2.00. Found: C, 92.66;

H, 5.28; N, 2.06.

Synthesis of 5',5''''-(9-phenyl-9H-carbazole-3,6-diyl)bis(([1,1':3',1''-terphenyl] -2'-carbonitrile)) (2(3phCN)-phCz)

2(3phCN)-phCz was prepared according to the same procedure as that for 3ph-phCz,and the target product was obtained as a yellow solid (0.83 g) with a yield of 62%. ^{1}H NMR (600 MHz, $CDCl_3$): δ = 8.52 (s, 2H), 7.86 (s, 4H), 7.79 (dd, J=8.6, 1.4, 2H), 7.72 (d, J=7.2, 8H), 7.68 (d, J=7.6, 2H), 7.61 (d, J=7.5, 2H), 7.56 (t, J=7.5, 10H), 7.51 (t, J=7.3, 5H). ^{13}C NMR (150 MHz, $CDCl_3$): δ = 146.36, 144.49, 140.61, 137.80, 135.85, 130.39, 129.13, 128.02, 127.70, 127.64, 127.09, 126.40, 125.90, 124.88, 122.92, 118.33, 117.22, 109.71, 107.22. MS (MALDI-TOF) [m/z]: Calcd for $C_{56}H_{35}N_3$, 749.28; Found, 749.29. Anal. Calcd. for $C_{56}H_{35}N_3$: C, 89.69; H, 4.70; N, 5.60. Found: C, 89.63; H, 4.75; N, 5.61.

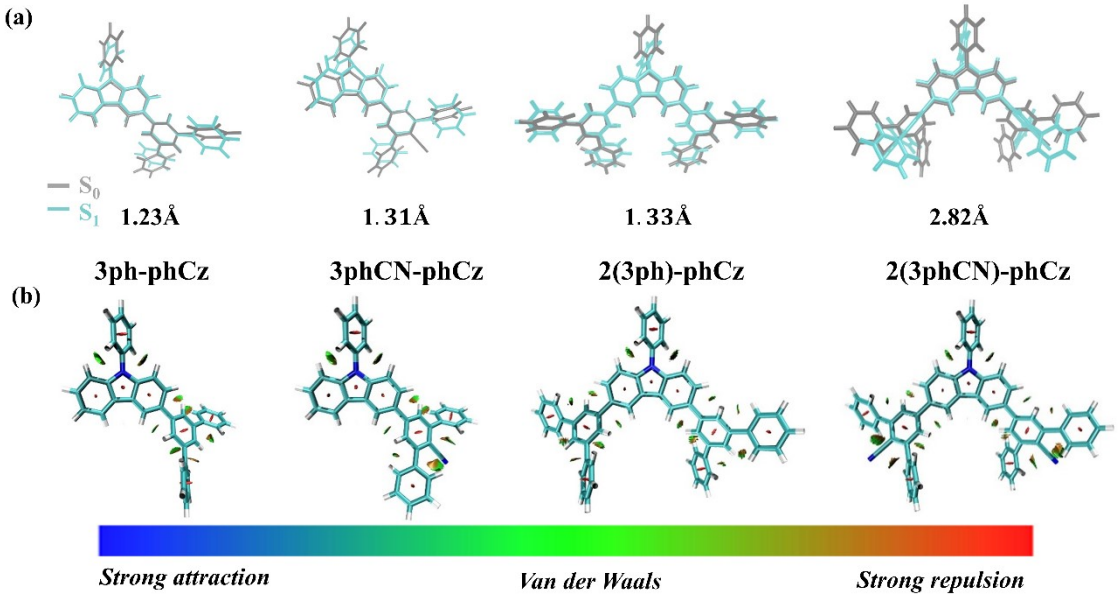

Figure S1. (a) Geometries of S_0 and S_1 and (b) Reduced density gradient isosurface maps of 3ph-phCz, 3phCN-phCz, 2(3ph)-phCz and 2(3phCN)-phCz.

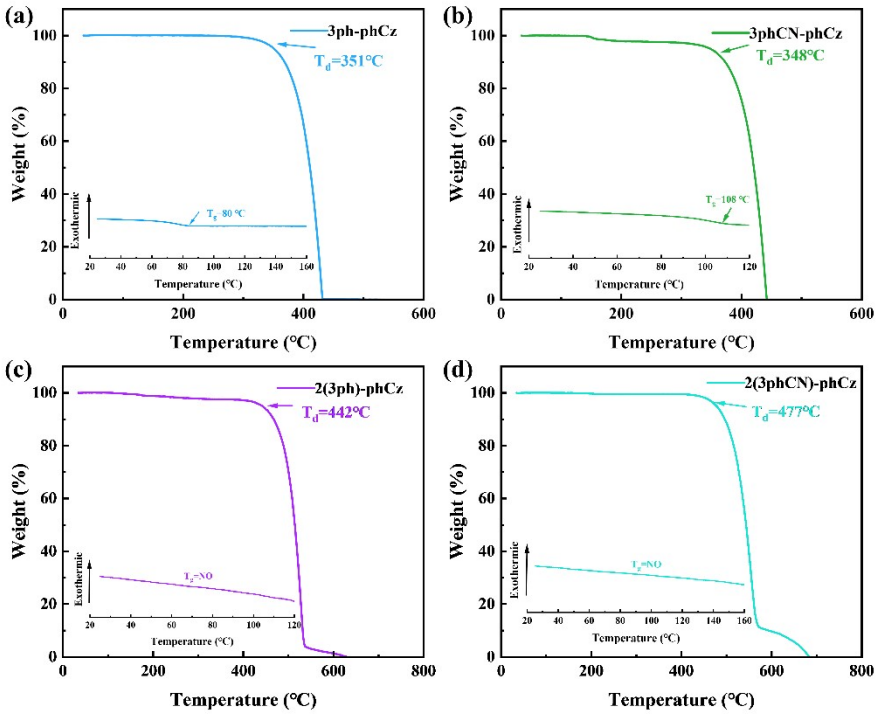

Figure S2. The TGA and DSC of the four compounds. (a) 3ph-phCz, (b) 3phCN-phCz, (c) 2(3ph)-phCz, (d) 2(3phCN)-phCz.

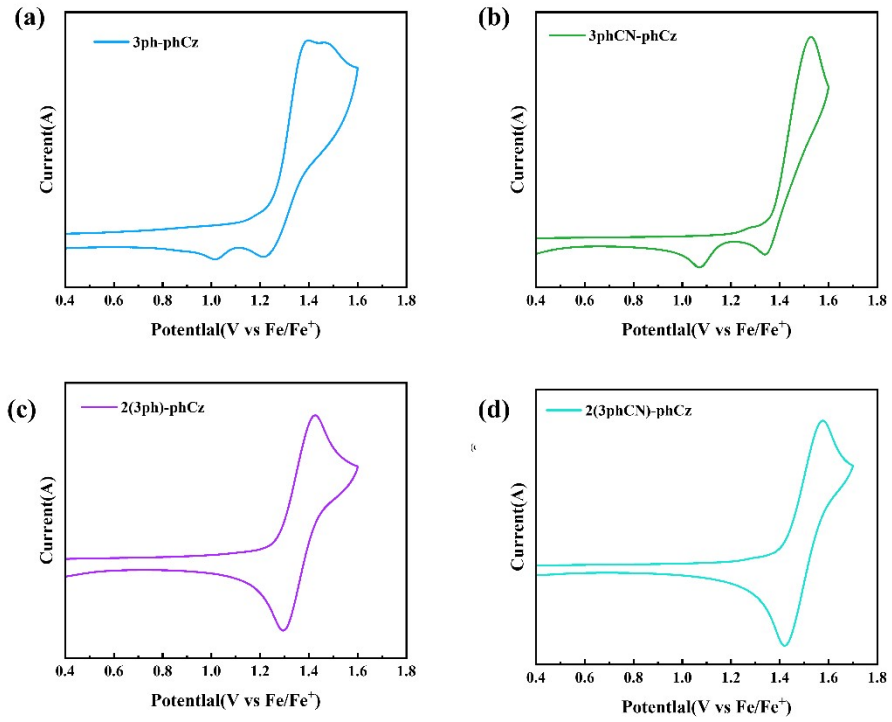

Figure S3. Cyclic voltammetry (CV) curves of 3ph-phCz, 3phCN-phCz, 2(3ph)-phCz and 2(3phCN)-phCz in CH_2Cl_2 for oxidation scan (vs. Fc/Fc^+).

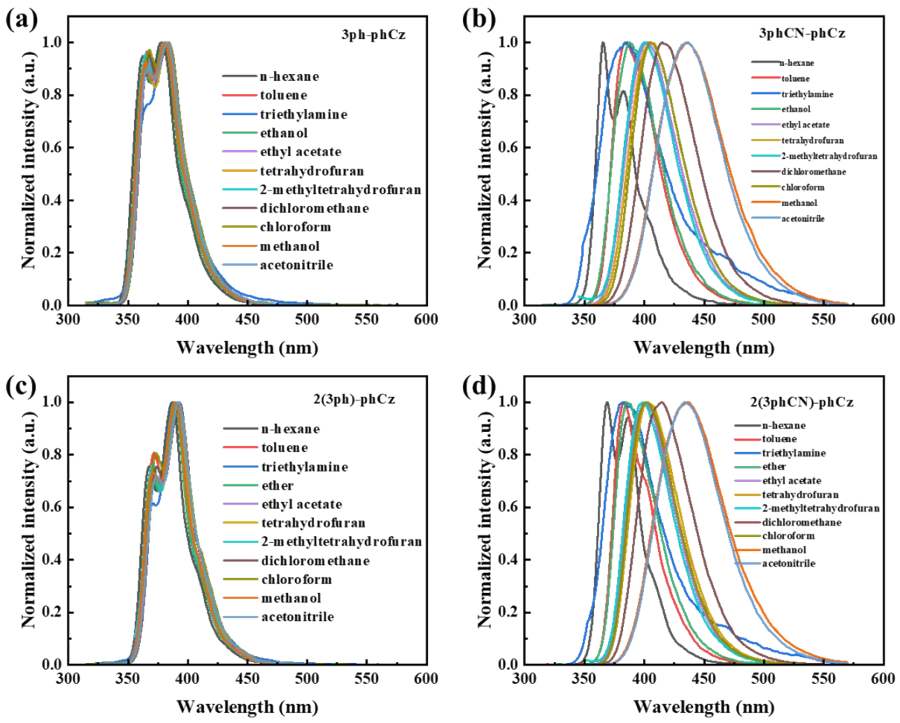

Figure S4. Normalized fluorescence spectra for (a) 3ph-phCz, (b) 3phCN-phCz, (c) 2(3ph)-phCz and (d) 2(3phCN)-phCz in different solvent at room temperature.

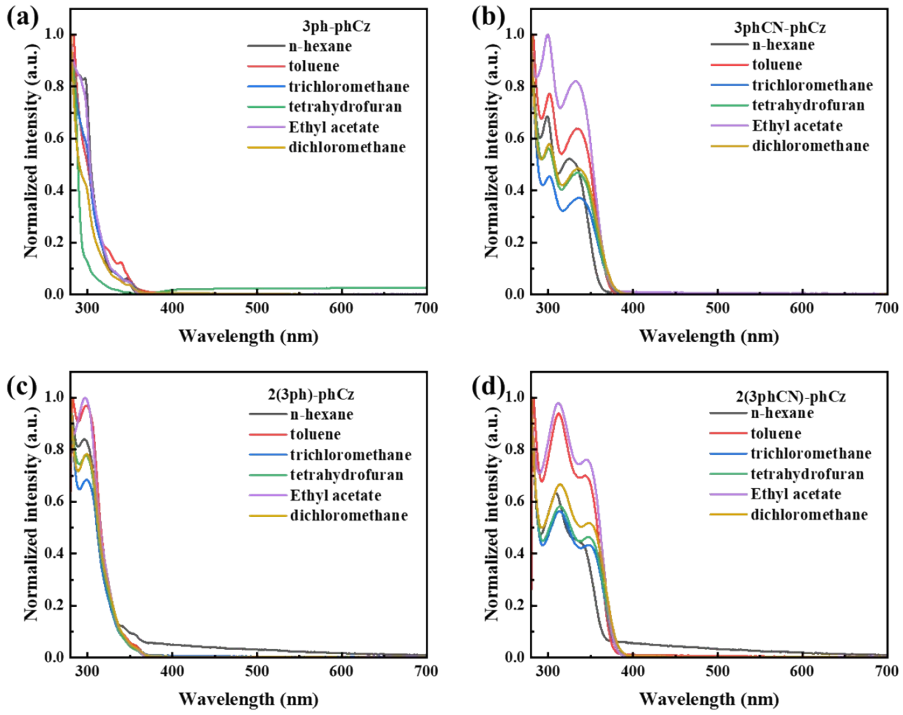

Figure S5. Normalized UV−vis absorption spectra for (a) 3ph-phCz, (b) 3phCN-phCz, (c) 2(3ph)-phCz and (d) 2(3phCN)-phCz in different solvent at room temperature.

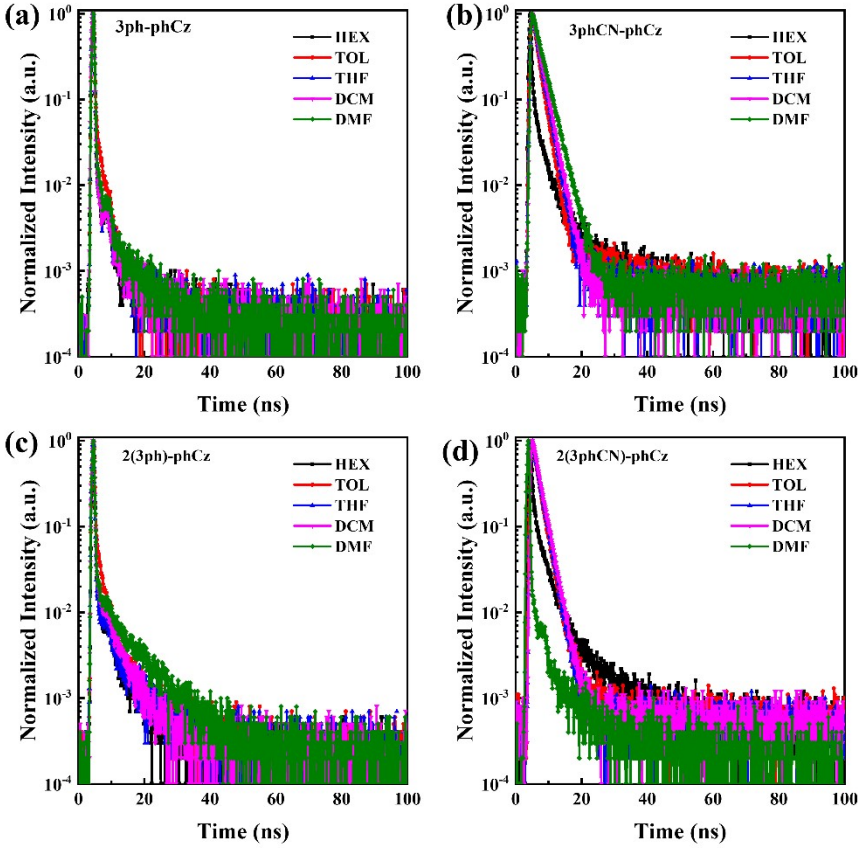

Figure S6. Normalized transient PL decay spectra at room temperature. (a) 3ph-phCz,

(b) 3phCN-phCz, (c) 2(3ph)-phCz and (d) 2(3phCN)-phCz in different solvent. (HEX: n-hexane, Tol: toluene, THF: tetrahydrofuran, DCM: dichloromethane, DMF: *N*, *N*-Dimethylformamide)

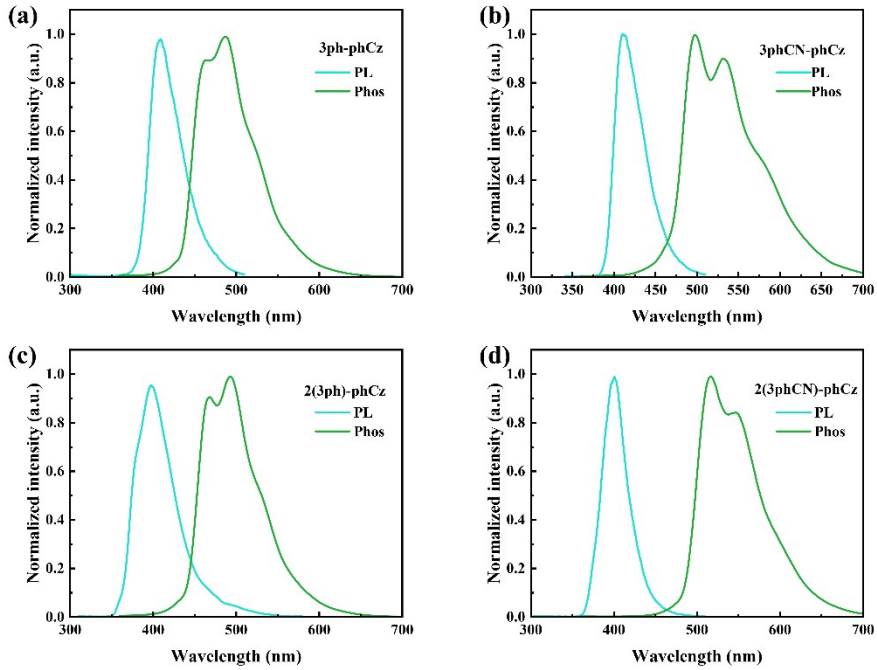

Figure S7. The photoluminescence (PL), phosphorescence (Phos) spectra of (a) 3ph-phCz, (b) 3phCN-phCz, (c) 2(3ph)-phCz and (d) 2(3phCN)-phCz in neat film.

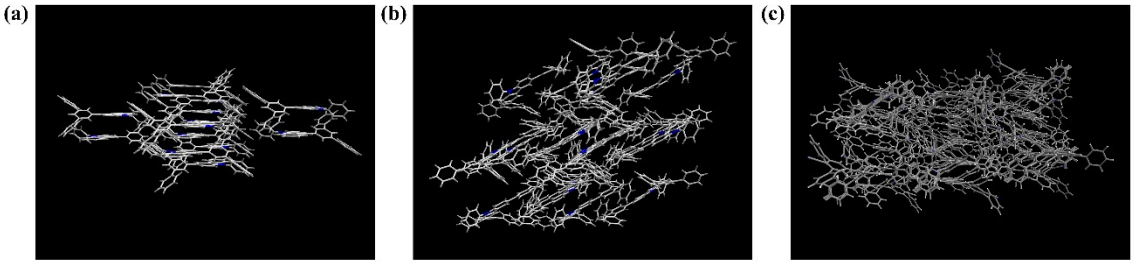

Figure S8. Crystal structures of (a) 3ph-phCz, (b) 2(3ph)-phCz and (c) 2(3phCN)-phCz.

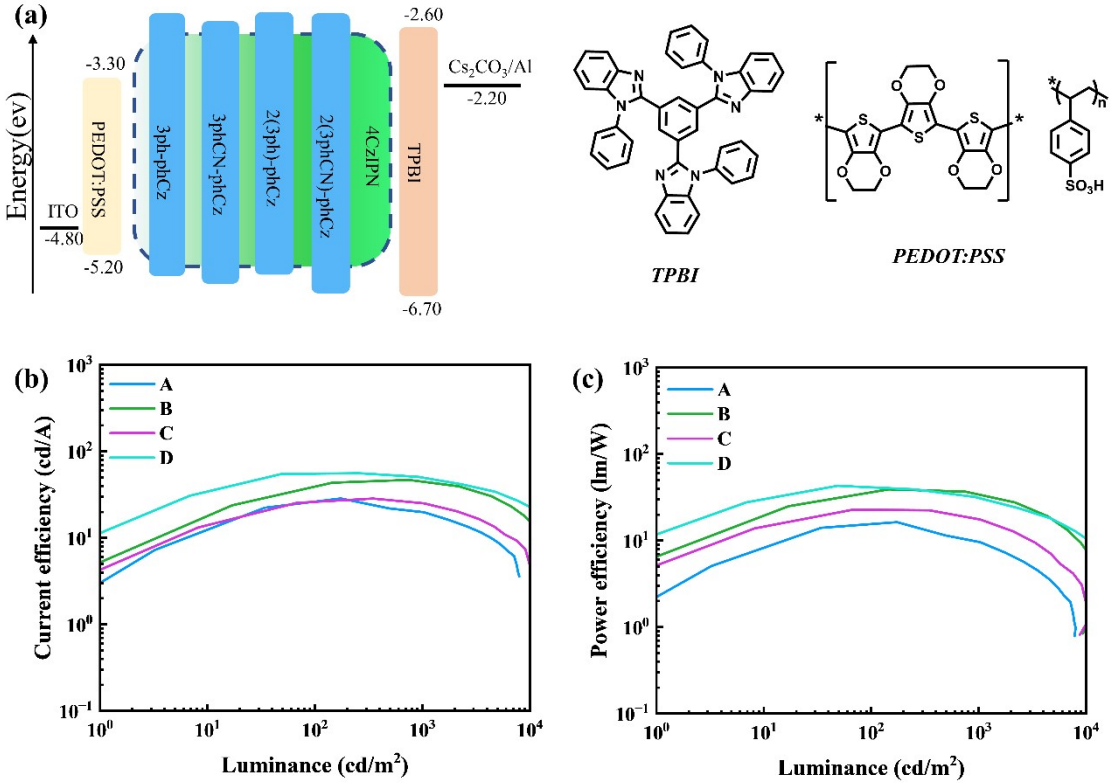

Figure S9. (a) The Device structure and energy diagram. (b) The curves of current efficiency (CE) versus luminance. (c) The curves of and power efficiency (PE) versus luminance.

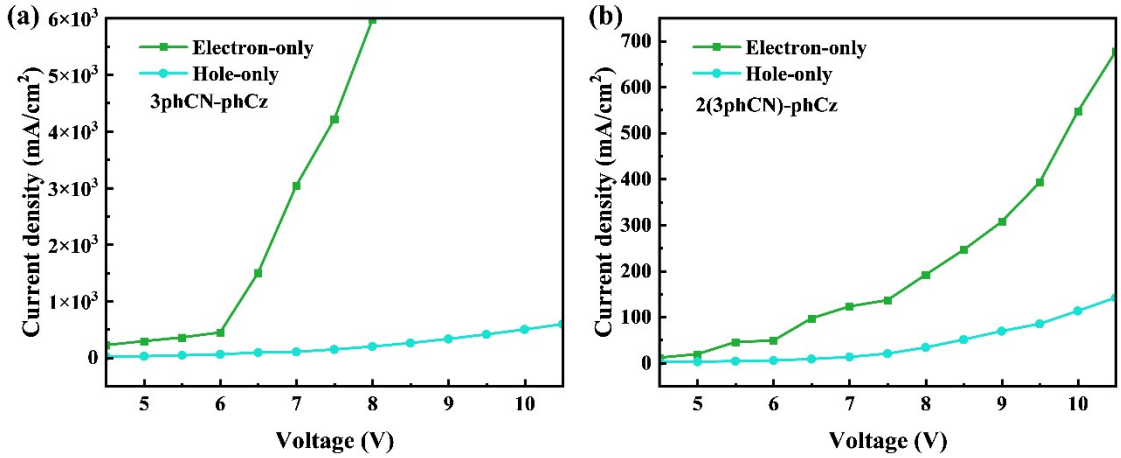

Figure S10. The IV characteristics of electron-only devices with a configuration of ITO|Al (50 nm)|EML (40 nm)|TBPI(30 nm) |Cs_2CO_3(2 nm) |Al (100 nm), and IV characteristics of hole-only devices with configurations of ITO|PEDOT:PSS (40 nm)|EML (40 nm)|MoO_3 (20 nm)|Al (100 nm) based on HLCT materials.

Table S1 Measured by DSC/TGA at a heating rate of 10 °C min^{-1}

	3ph-phCz	3phCN-phCz	2(3ph)-phCz	2(3phCN)-phCz
T_d/°C	351	348	442	477
T_g/°C	80	108	-	-

Table S2 Spectral Properties of 3ph-phCz, 3phCN-phCz, 2(3ph)-phCz and 2(3phCN)-phCz in various solutions.

	3ph-phCz		3phCN-phCz		2(3ph)-phCz		2(3phCN)-phCz	
	λ_{abs}[a]	λ_{em}[b]	λ_{abs}[a]	λ_{em}[b]	λ_{abs}[a]	λ_{em}[b]	λ_{abs}[a]	λ_{em}[b]
	[nm]	[nm]	[nm]	[nm]	[nm]	[nm]	[nm]	[nm]
HEX	347	362/378	325	366/382	297	368/387	335	369/387
TOL	340	366/382	330	384	299	372/391	344	384
TCM	348	368/383	336	405	299	373/392	347	402
THF	349	366/383	335	406	298	372/391	348	403
EA	347	365/381	332	403	297	371/390	345	402
DCM	349	367/384	334	414	299	374/392	347	415

λ_{abs}[a] is the maximum absorption wavelength. λ_{em}[b] is the peak of fluorescence. (HEX: n-hexane, TOL: toluene, TCM: trichloromethane, THF: tetrahydrofuran, EA: ethyl acetate, DCM: dichloromethane).

Table S3 Crystal Date and structures Refinements of 3ph-phCz, 2(3ph)-phCz and 2(3phCN)-phCz

	3ph-phCz	**2(3ph)-phCz**	**2(3phCN)-phCz**
CCDC Number	2311136	2311138	2311137
Empirical formula	$C_{36}H_{25}N$	$C_{54}H_{37}N$	$C_{56}H_{25}N_3$
Formula weight	471.57	699.85	749.87
Crystal system	Triclinic	Triclinic	monoclinic
T(K)	100	100	100
Space group	P-1	P-1	$P2_1/C$
a/ Å	8.5778(2)	13.96660(10)	14.1524(2)
b/ Å	9.7514(2)	14.11200(10)	21.4405(3)
c/ Å	16.0559(3)	20.4883(2)	27.9631(5)
α/°	93.256(2)	92.6390(10)	90
β/°	99.424(2)	101.3210(10)	91.7180(10)

γ/°	110.502(2)	91.0570(10)	90
V/ Å^3	1228.58(5)	3953.85(6)	8481.2(2)
Z	2	4	8
Density, g/cm^3	1.275	1.176	1.175
F (000)	496.0	1472.0	3136.0
GOF	1.062	1.052	1.081

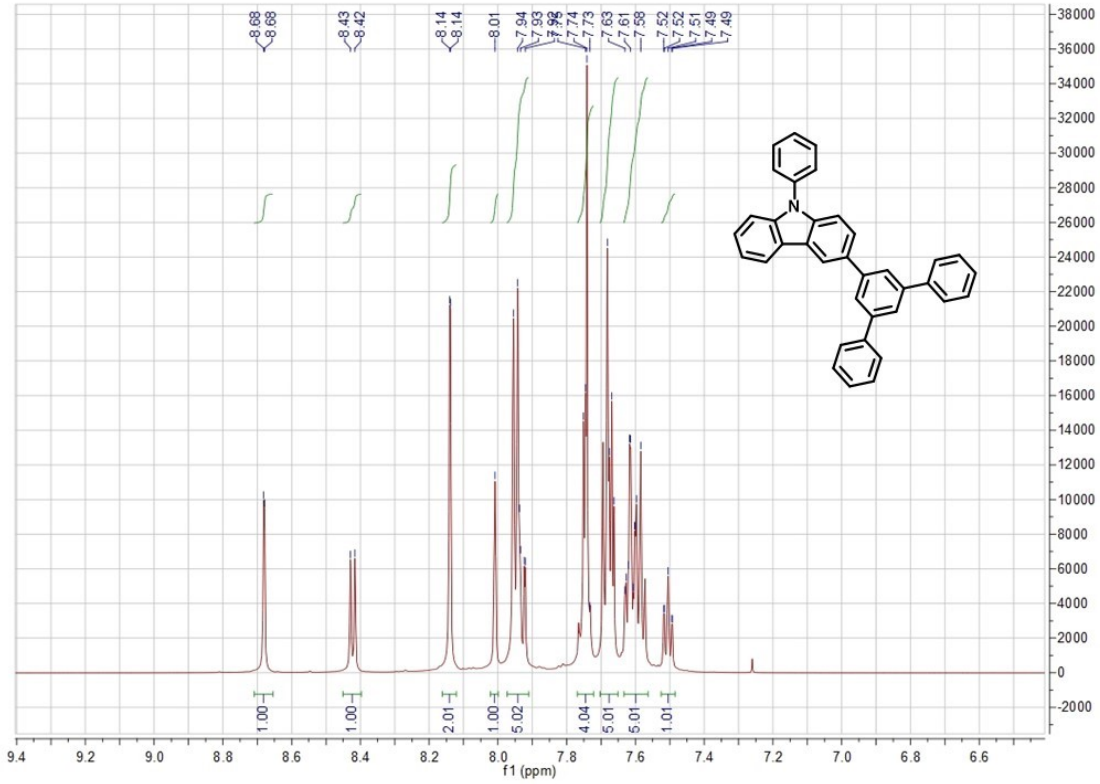

Figure S11. ^{1}H NMR spectra of 3ph-phCz.

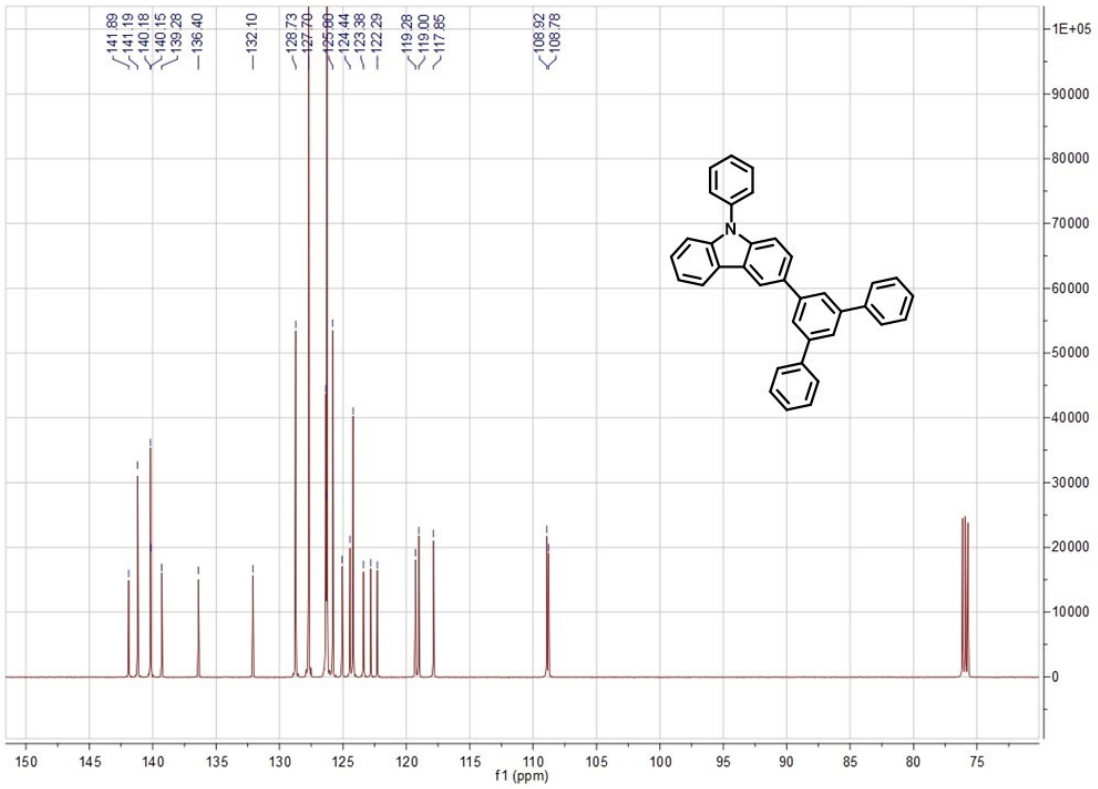

Figure S12. ^{13}C NMR spectra of 3ph-phCz.

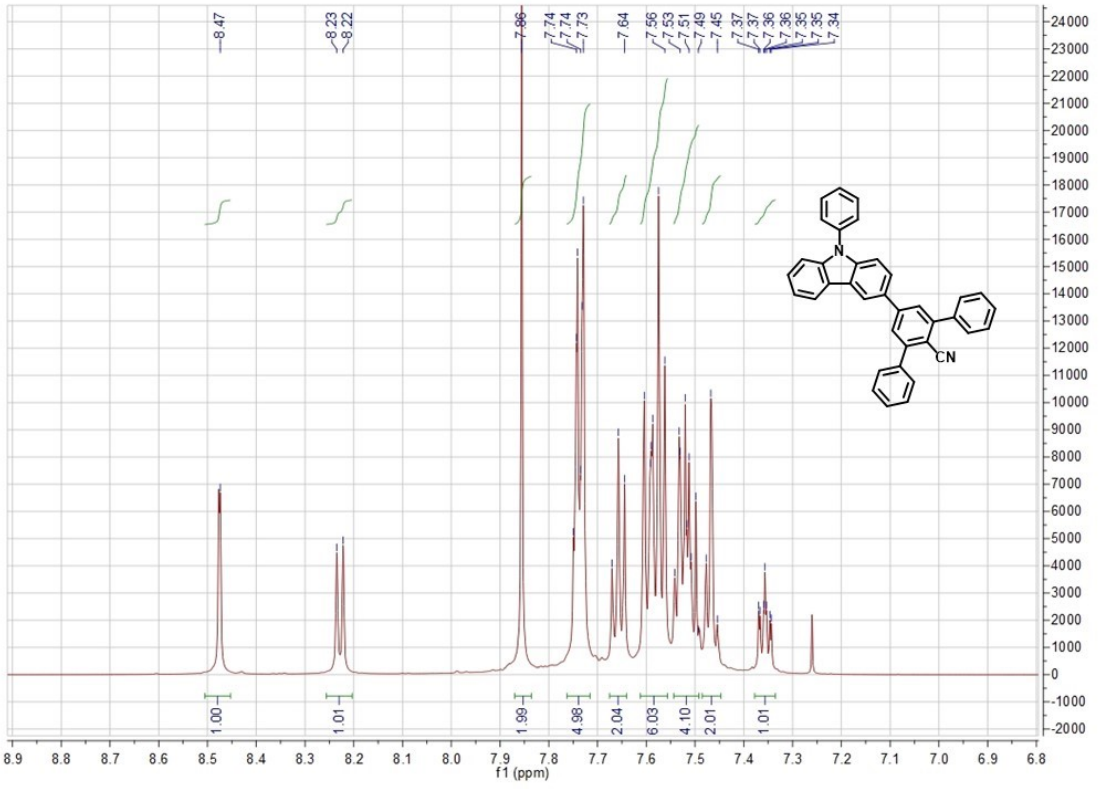

Figure S13. ^{1}H NMR spectra of 3phCN-phCz.

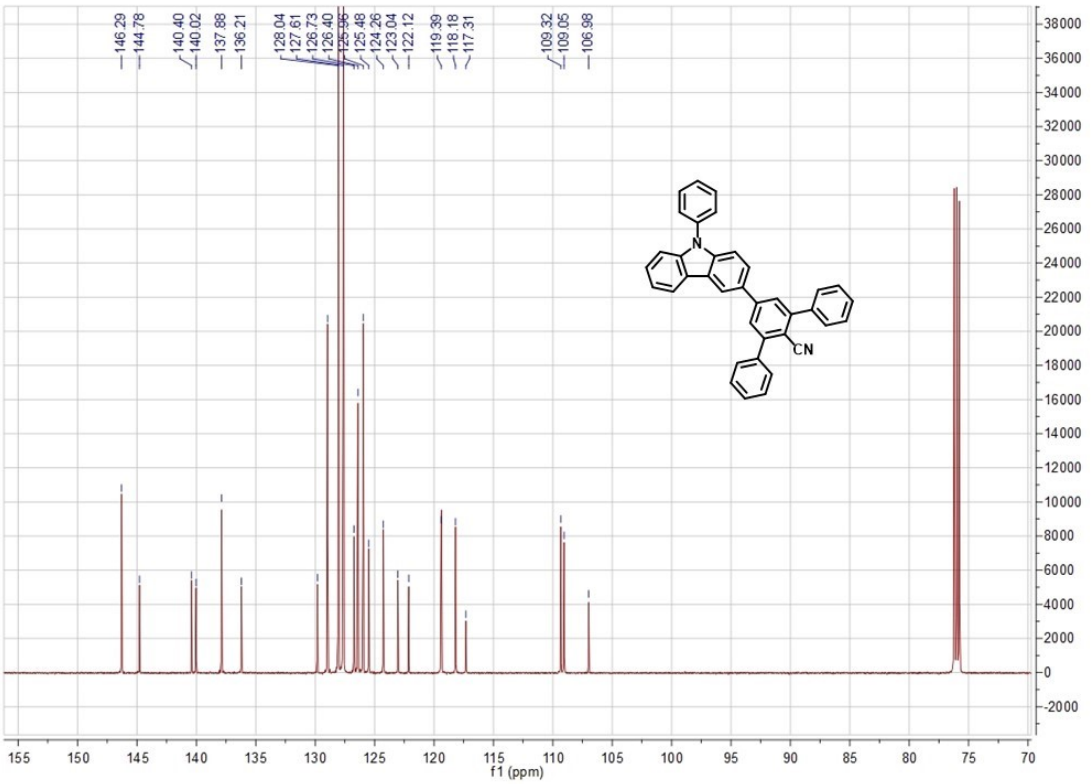

Figure S14. ^{13}C NMR spectra of 3phCN-phCz.

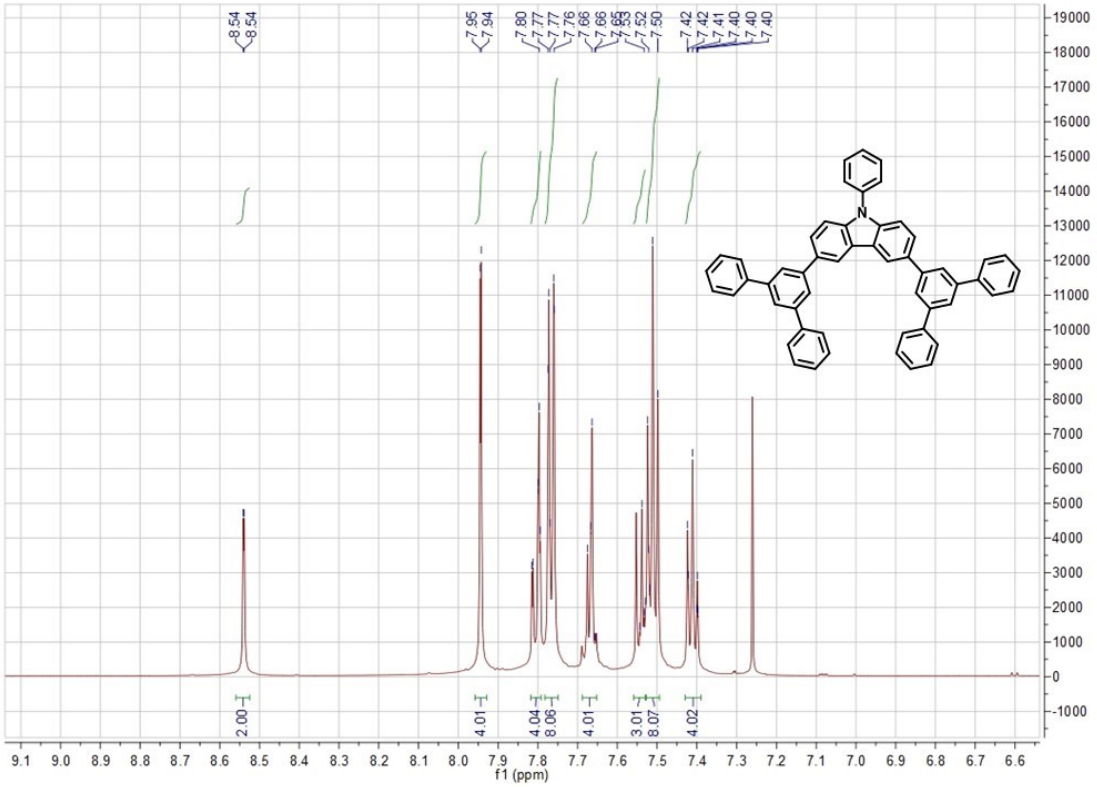

Figure S15. ^{1}H NMR spectra of 2(3ph)-phCz.

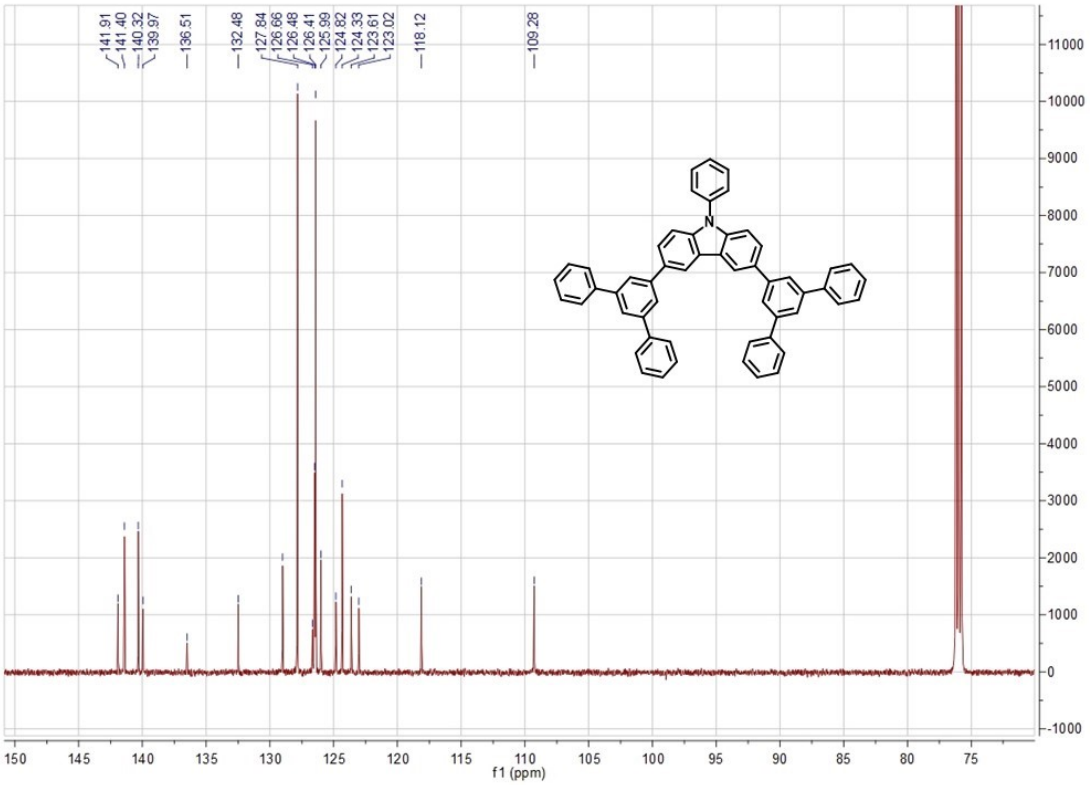

Figure S16. ^{13}C NMR spectra of 2(3ph)-phCz.

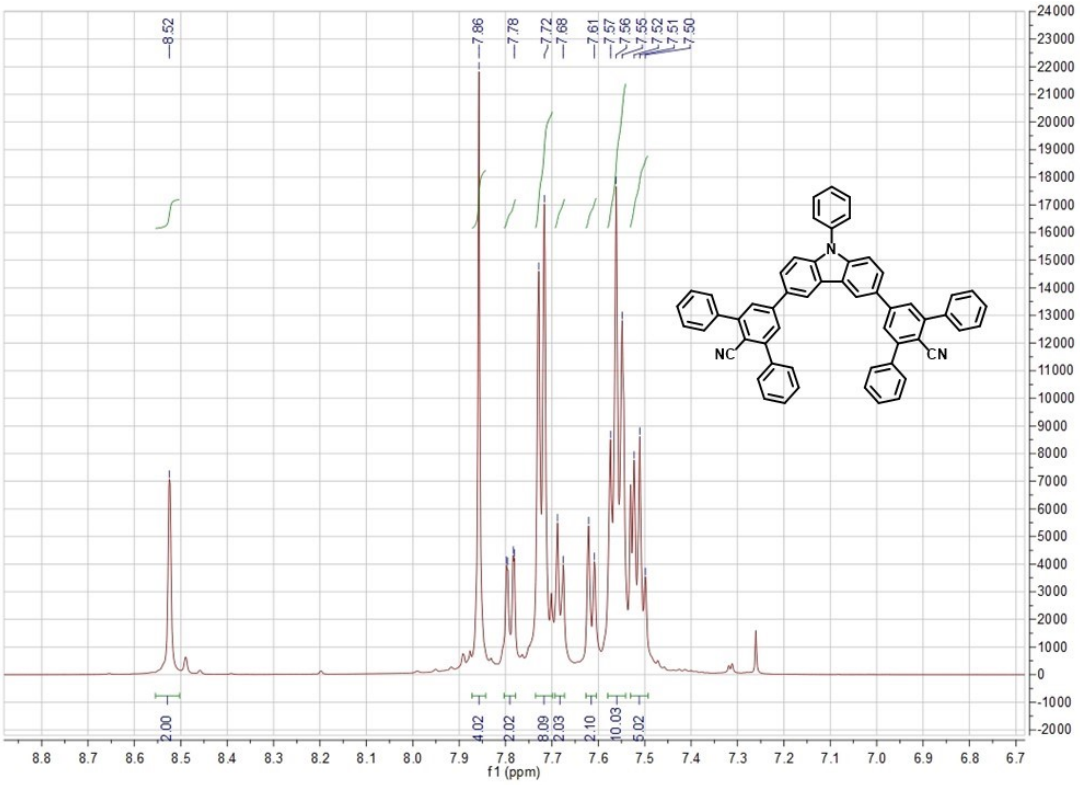

Figure S17. ^{1}H NMR spectra of 2(3phCN)-phCz.

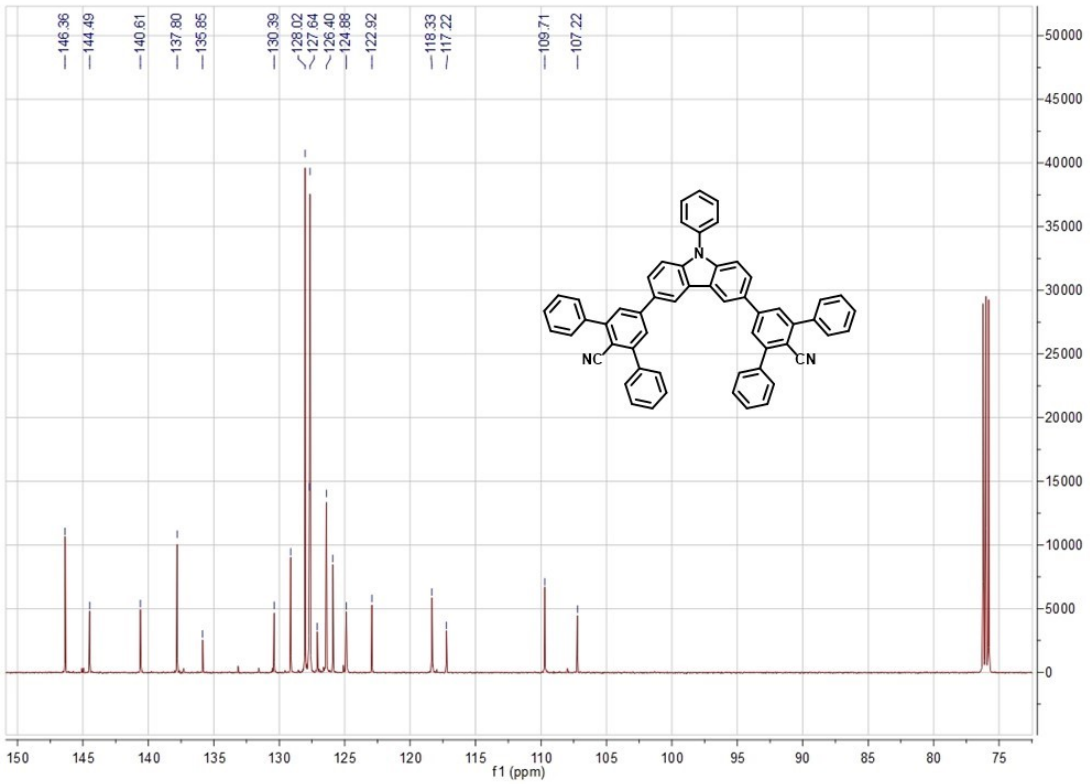

Figure S18. ^{13}C NMR spectra of 2(3phCN)-phCz.

Reference

1. Z. R. Grabowski, K. Rotkiewicz and W. Rettig, *Chemical Reviews*, 2003, **103**, 3899-4032.
2. X. Tang, Q. Bai, Q. Peng, Y. Gao, J. Li, Y. Liu, L. Yao, P. Lu, B. Yang and Y. Ma, *Chemistry of Materials*, 2015, **27**, 7050-7057.
3. H. Zhang, B. Zhang, Y. Zhang, Z. Xu, H. Wu, P.-A. Yin, Z. Wang, Z. Zhao, D. Ma and B. Z. Tang, *Advanced Functional Materials*, 2020, **30**, 2002323.